Superhardness, stability, and metallicity of diamondlike BC$_5$: Density functional calculations

Yongcheng Liang,[1,2] Wenqing Zhang,[1] Jianzhi Zhao,[3] and Lianfeng Chen[1]

[1]*State Key Laboratory of High Performance Ceramics and Superfine Microstructures, Shanghai Institute of Ceramics,*
Chinese Academy of Sciences, Shanghai 200050, China
[2]*College of Engineering Science and Technology, Shanghai Ocean University, Shanghai 201306, China*
[3]*Beijing National Laboratory for Condensed Matter Physics and Institute of Physics, Chinese Academy of Sciences,*
Beijing 100080, China

The recently synthesized diamondlike BC$_5$ (*d*-BC$_5$) was shown to own a few interesting physical properties, which are yet to be confirmed due to the difficulty in the synthesis of adequately sized single crystals. Our density functional calculations not only confirm *d*-BC$_5$ to be an ultraincompressible and superhard material, but also reveal that it exhibits mechanical stability and metallic behavior. The higher energy barrier of *d*-BC$_5$ (0.057 eV/atom higher than diamond) implies that *d*-BC$_5$ is about 500 K more kinetically stable than diamond. Moreover, the trend that the mechanical properties drop with the increasing of boron content in diamondlike B-C compounds (*d*-BC$_x$) can be understood through analyzing the electronic structures. The combination of high hardness, strong stiffness, large activation barrier, and metallic feature allows this series of *d*-BC$_x$ promising applications as advanced abrasives and electronic devices at high temperature and high-pressure conditions.

Diamond is widely accepted as the hardest material available in nature, but it is not used to cut iron and other ferrous metals due to the detrimental formation of iron carbide during high-speed machining.[1] New superhard materials are thus not only of great scientific interest, but also of practical importance. Years of synthetic and theoretical efforts[2–12] have been devoted to hunting for new diamondlike B-C-N-O phases with more thermal and chemical stability. Very recently, Solozhenko *et al.*[13] have synthesized *d*-BC$_5$ with the ultimate boron solubility in diamond. They reported that the *d*-BC$_5$ has high bulk modulus (335 GPa), extreme Vickers hardness (71 GPa), high-thermal stability (up to 1900 K) and conductive character. As we know, most of the superhard materials are insulators or semiconductors with covalent bonds. Hardness depends strongly on plastic deformation, which results in electron-pair bonds being broken and remade in a covalent crystal. Breaking an electron-pair bond means that two electrons become energetically excited from the valence band to the conduction band, so the hardness of a material is often related to its electronic structure, particularly to the band gap.[14] It therefore is a bit surprising that a conductive system is so hard. Moreover, because of the technical difficulties, no adequately sized single crystals may be obtained, and thus its interesting physical properties need to be confirmed theoretically. On the other hand, density functional calculations can provide accurate and reliable predictions of mechanical properties to validate these experimental values. In particular, theoretical understanding and interpretation of relative stability and conductive character is also of great importance. Therefore, the first-principles calculations that can provide further details and theoretical evidence about mechanical and electronic properties are highly demanded.

In this paper, we investigate the mechanical and electronic properties of *d*-BC$_5$ using density functional calculations. At the same time, in order to insight into relative stability, we calculate their energy difference, energy barrier and transi-

tion pressure of *d*-BC$_5$ relative to graphitelike BC$_5$ (*g*-BC$_5$). To fully explore the trends of these physical properties in this species of *d*-BC$_x$ compounds, diamond and *d*-BC$_7$ are also systematically studied for comparison. Our results indicate that *d*-BC$_5$ is not only ultra-incompressible and superhard, but also exhibits mechanical stability, relatively high-energy barrier and metallic behavior. The mechanical properties of diamond, *d*-BC$_7$, and *d*-BC$_5$ are also found to slightly drop with the B-content increasing.

Our calculations are performed for diamond, *d*-BC$_7$, *d*-BC$_5$, graphite, *g*-BC$_7$ and *g*-BC$_5$ by employing the BSTATE code[15] using the plane-wave basis pseudopotential method. Local density approximation (LDA)[16] and generalized gradient approximation (GGA)[17] are used as the exchange-correlation energy functional. The 2*s*- and 2*p*-states of B and C are treated by the Vanderbilt ultrasoft pseudopotentials.[18] Due to the small energy differences between *d*-BC$_x$ and *g*-BC$_x$, we perform a very careful check for the convergence of calculated results with respect to the number of *k*-points and the cutoff energy for the plane-wave expansion of the wave function. Finally, we adopt a cutoff energy of 36 Ry for all the systems and Monkhorst-Pack[19] k-points generated with $12 \times 12 \times 12$, $12 \times 12 \times 12$, $12 \times 12 \times 6$, $13 \times 13 \times 7$, $11 \times 11 \times 7$, and $9 \times 9 \times 7$ mesh parameter grids for diamond, *d*-BC$_7$, *d*-BC$_5$, graphite, *g*-BC$_7$, and *g*-BC$_5$, respectively, to obtain good convergence of 0.001 eV in absolute total energy. The description of methods obtaining the related mechanical properties refers to our previous works.[20–22]

Because of their similar atomic numbers, diffraction cannot distinguish between boron and carbon atoms, and thus, the synthesized *d*-BC$_5$ was experimentally interpreted a pseudocubic structure ($a=3.635$ Å).[13] In fact, *d*-BC$_5$ adopts a hexagonal structure, which is compatible with a cubic symmetry for $c/a = \sqrt{6}$. Based on the theoretical atomic structure of Calandra *et al.*,[23] we perform a structural search and optimization. Lattice constants of the optimized hexagonal
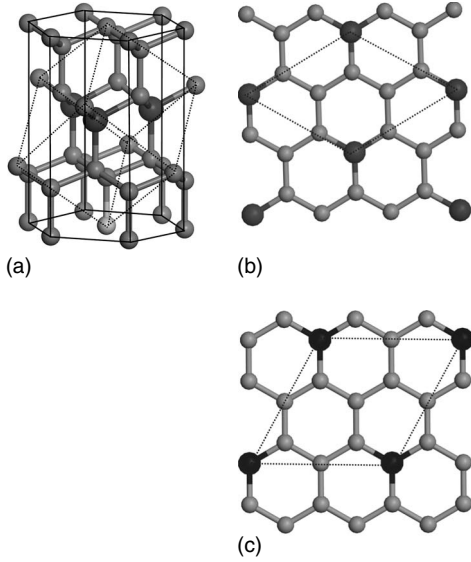
FIG. 1. Crystal geometry of (a) d-BC$_5$, (b) g-BC$_5$, and (c) g-BC$_7$. The dark big and gray small spheres represent the boron and carbon atoms, respectively. In (a) the solid and dashed lines show the hexagonal and pseudocubic unit cells, respectively. The (b) and (c) hexagonal sheets form g-BC$_5$ and g-BC$_7$ by AB stacking, respectively.

d-BC$_5$ within the LDA (GGA) are $a=2.522(2.552)$ Å and $c=6.324(6.392)$ Å. Structures shown in Fig. 1(a) are optimized geometries, in which the pseudocubic cell has 2.3% elongation along the (111) axis. In the case of the structure d-BC$_7$, we adopt the eight-atom diamond unit cell with one B atom substituting one C atom. For the g-BC$_5$ and g-BC$_7$ structures considered here, the B atoms are contained as hexagonal units within the graphite planes, as shown in Figs. 1(b) and 1(c), and with AB stacking of these planes.[24]

Table I lists the calculated equilibrium volume, nearest-neighbor distance, bulk modulus, and its pressure derivative of diamond, d-BC$_7$ and d-BC$_5$. From this table, it can be seen that with the increasing of B content, the volume and nearest-neighbor distance increase while the bulk modulus steadily decreases. For diamond and d-BC$_7$, our results are in

TABLE I. Calculated equilibrium volume V_0 (Å^3/atom), nearest neighbor distance d_0 (Å^3), bulk modulus B_0 (GPa) and its pressure derivative (B'_0), compared with available data for diamond, d-BC$_7$ and d-BC$_5$.

Material	Method	V_0	d_0	B_0	B'_0
Diamond	LDA	5.508	1.529	469	3.59
	GGA	5.693	1.546	435	3.66
	Expt.[a]	5.673	1.545	446	3.0
d-BC$_7$	LDA	5.733	1.550	417	3.58
	GGA	5.933	1.568	387	3.66
d-BC$_5$	LDA	5.805	1.595	407	3.58
	GGA	6.006	1.612	379	3.62
	Expt.[b]	6.004	1.608	335	4.5

[a]Reference 25.
[b]Reference 13.

good agreement with other theoretical or experimental data[11,25] within the LDA and GGA errors, substantiating the validity of our calculations. For d-BC$_5$, although the experimental equilibrium volume accords with ours, the experimental value (335 GPa) underestimates the bulk modulus by 15% with comparison to the average of our results (393 GPa) with LDA and GGA, showing that it is an ultraincompressible material.

In order to further gain insight into their elastic stability and mechanical properties, elastic constants, shear moduli, Young's moduli, and Poisson's ratios of the three d-BC$_x$ crystals are presented in Table II. According to the Born-Huang elastic stability criterion,[26] diamond, d-BC$_7$, and d-BC$_5$ are all mechanically stable, which accord with the experimental conclusion[13] that there exists a continuous series of diamondlike BC$_x$ solid solution (in the range of $x \geqslant 5$). Also, we can find that the linear incompressibility (Young's modulus) and shear resistance (shear modulus and elastic constant C_{44}) slightly drop from diamond, to d-BC$_7$, then to d-BC$_5$. For d-BC$_5$, the shear modulus and the elastic constant C_{44}, indirect measuring the hardness, are calculated to be 410 (386) GPa and 401 (382) GPa with the LDA (GGA), respectively. These values are exceptionally high, approaching 70% of those of the hardest diamond and rivaling to c-BN ($G=403$ GPa, $C_{44}=479$ GPa).[27] However, the dependence of hardness on bulk or shear modulus is not unequivocal and monotonic, and thus a quantitative estimate is essential. The theoretical hardness of crystals can be estimated from the semiempirical theory,[14,28,29] in which the hardness can be described by the valence electron density, bond length, and ionicity. For d-BC$_5$, five different bond lengths d_{12}(B-C)=1.608 Å, d_{16}(B-C)=1.623 Å, d_{32}(C-C) $=d_{34}$(C-C)=1.54 Å, d_{54}(C-C)=1.55 Å, d_{56}(C-C)=1.49 Å and the parameters e_1(B)=2.910 and e_2(C)=4.082, e_3(C) =4.095, e_4(C)=4.077, e_5(C)=4.107, and e_6(C)=4.020 are evaluated by the first-principles calculations. Applying the Eq. (5) in Ref. 29, the predicted hardness of d-BC$_5$ is about 63 GPa, which agrees with the measured value (71 GPa). Therefore, the present calculations clearly show that d-BC$_5$ is a superhard material.

We turn to the stability of d-BC$_x$ relative to g-BC$_x$. Because of the fact that LDA or GGA inaccurately describe van der Waals interactions between the layers in graphite, g-BC$_5$ and g-BC$_7$, test calculations for graphite are performed first. For graphite crystal we carry out three kinds of calculations: (1) optimizing the c/a ration with LDA, (2) optimizing the c/a ration with GGA, and (3) fixing the c/a ratio as experimental result of 2.724 with GGA. The obtained results of three cases are compared with the previous calculations and experiments.[30–32] The calculation of case (1) well predict the equilibrium volume (8.631 Å^3/atom) and bulk modulus (37 GPa) of graphite, but do not get reasonable energy ordering between graphite and diamond, which are consistent with the results of Ribeiro *et al.*[31] Although the calculation of case (2) correctly show that the equilibrium energy of graphite is lower than the equilibrium energy of diamond, they vastly overestimate the crystal structure (9.804 Å^3/atom), especially the c-axis (c/a=3.032), and underestimate the energy barrier (0.116 eV/atom). For the calculation of case (3) in Fig. 2(a), we obtain that diamond is higher in energy by

TABLE II. Calculated elastic constants C_{ij} (GPa), shear modulus G (GPa), Young's modulus E (GPa), and Poisson's ratio υ for diamond, graphite, d-BC$_7$, g-BC$_7$, d-BC$_5$, and g-BC$_5$.

Material	Method	C_{11}	C_{12}	C_{13}	C_{33}	C_{44}	G	E	υ
Diamond	LDA	1106	151			604	550	1186	0.079
	GGA	1053	127			565	522	1119	0.072
Graphite	LDA	1121	179	−2.4	24	4.2	122	291	0.191
	GGA	1001	154	−1.8	17	2.1	107	255	0.190
d-BC$_7$	LDA	807	222			537	421	945	0.122
	GGA	769	196			498	399	891	0.116
g-BC$_7$	LDA	923	188	−0.56	25	3.3	93	228	0.223
	GGA	904	188	−0.53	19	2.7	94	227	0.210
d-BC$_5$	LDA	931	194	69	1164	401	410	922	0.125
	GGA	865	177	64	1086	382	386	865	0.121
g-BC$_5$	LDA	894	199	2.3	32	4.3	95	232	0.222
	GGA	842	195	0.19	20	0.81	84	206	0.227

0.120 eV/atom than graphite, that the energy barrier of diamond is 0.322 eV/atom relative to graphite, and that the transition pressure from graphite to diamond is 6.2 GPa. These values accord with the previously calculations and experiments.[33,34] However, the calculation of the case (3) gives the unreasonable bulk modulus (273 GPa) of graphite. Thus, we rationally believe that the calculations of the cases (1) and (2) are better than that of the case (3) for elastic properties of g-BC$_x$, whereas the calculation of case (3) is better for energy barriers. For graphite, g-BC$_7$ and g-BC$_5$, their elastic constants, shear moduli, Young's moduli, and Poisson's ratios have been calculated using the cases (1) and (2) methods, and their values are listed in Table II. It is found that their main mechanical properties (C_{11}, G, and E) drop with the increasing of boron content in g-BC$_x$ compounds. However, it should be stressed that some values measuring interlayer interactions must be treated with some caution due to the LDA's inaccurate description of the van der Waals effect.

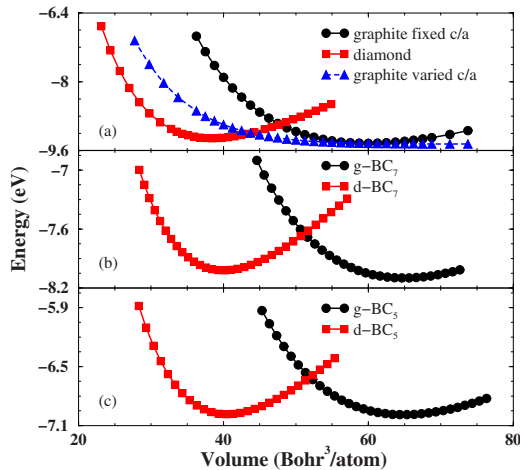For the energy difference, energy barrier and transition

FIG. 2. (Color online) Total energy vs volume curves of (a) diamond and graphite, (b) d-BC$_7$ and g-BC$_7$, and (c) d-BC$_5$ and g-BC$_5$ within the GGA calculations.
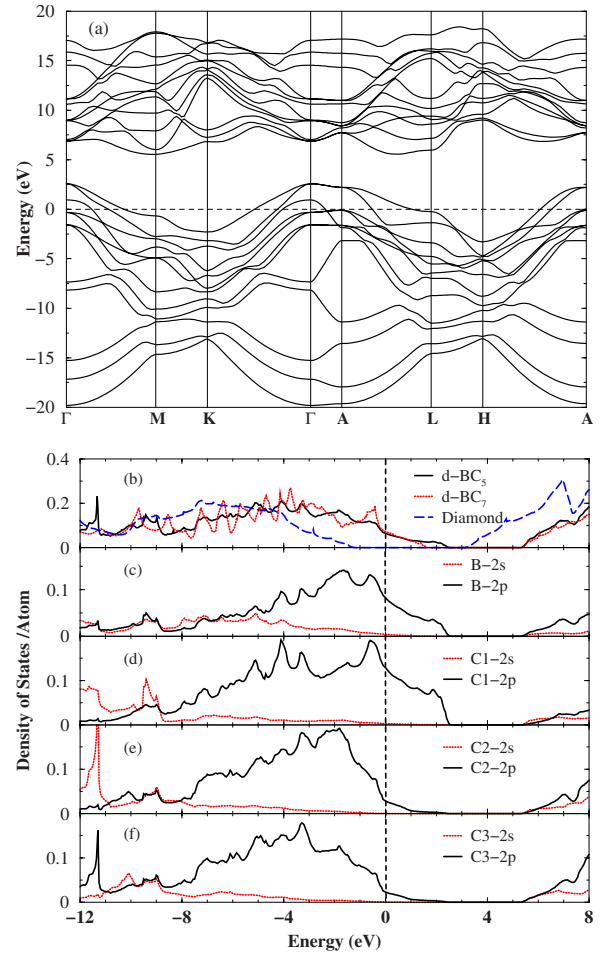

FIG. 3. (Color online) (a) Band structure of d-BC$_5$ from the GGA calculation. $\Gamma=(0,0,0)$, $M=(0.5,0,0)$, $K=(1/3,1/3,0)$, $A=(0,0,0.5)$, $L=(0.5,0,0.5)$, $H=(1/3,1/3,0.5)$. The Fermi level is indicated by a vertical dashed line. (b) Total DOS of d-BC$_5$, d-BC$_7$ and diamond. (c)–(d) Projected DOS of B, C1, C2, and C3 of d-BC$_5$, respectively.

pressure of d-BC$_x$ relative to g-BC$_x$, we therefore fix their c/a ratios as the experimental values[35] to calculate g-BC$_x$ with GGA. Figure 2 shows the calculated total energy as a function of volume for d-BC$_x$ and g-BC$_x$. From Figs. 2(b) and 2(c), we find that, with the B-content increasing in d-BC$_x$, the energy differences and transition pressures decrease while the energy barriers enhance. The energy differences of d-BC$_7$ and d-BC$_5$ relative to g-BC$_7$ and g-BC$_5$ are 0.078 and 0.004 eV/atom, respectively, and the corresponding transition pressures are obtained to be 3.9 and 0.5 GPa, respectively. For d-BC$_7$ and d-BC$_5$, our calculations predict the energy barriers of 0.374 and 0.379 eV/atom, respectively. The higher energy barrier of d-BC$_5$ (0.057 eV/atom higher than diamond) explains the experimental observation[13] that d-BC$_5$ is about 500 K more thermally stable than diamond.

We finally study the electronic structure of d-BC$_5$. The calculated band structure and total density of states (DOS) of hexagonal d-BC$_5$ are showed in Figs. 3(a) and 3(b), respectively. As can be seen, sp^3 hybrids of boron or carbon form into bonding states (from −20 to 3 eV) and antibonding states (above 5 eV). The lower 12 bands are attributed to the bonding states while the upper 12 bands belong to the antibonding states. Furthermore, there are three bands cross the Fermi level, indicating metallic feature in d-BC$_5$. It is because the charges of this system are not balanced due to the electron deficiency of boron atoms and not all the sp^3-hybridized bonding states are fully occupied with the appearance of some empty orbits above the Fermi level, similar to t-BC$_3$ of Liu $et~al.$[36] In d-BC$_5$ system, each boron has four carbon nearest neighbors (NNs): three carbon (called C1) with the bond length of 1.623 Å and one carbon (C2) with bond length of 1.608 Å. Other carbon atoms without NN boron bonding are called C3. To explain the contribution of different atoms to the formation of the empty orbits, we have calculated the 2s and 2p projected DOS of B, C1, C2, and C3, shown in Figs. 3(c)–3(f). We find that the empty orbits above the Fermi level are dominated by the B-2p and C1-2p states with a rather small contribution from

the C2- and C3-2p states. In other words, the sp^3-hybridized orbits with the longer B-C are partially filled, which results in the metallic behavior in d-BC$_5$.

It is obvious that strong covalent bonds and high-symmetrical structure are critical for high hardness of diamond. However, the hardness of boron-substituted diamond become to drop. In order to understand the mechanical trends of diamond, d-BC$_7$ and d-BC$_5$, we elucidate their total DOS in Fig. 3(b). For diamond, the bonding states are fully occupied while the antibonding states are unoccupied. For d-BC$_7$ and d-BC$_5$, the bonding states are not fully occupied since boron has one less electron than carbon, which results in the drop of mechanical properties with the B-content increasing. In addition, the bond lengths increase and the valence electron concentrations drop from diamond, d-BC$_7$ to d-BC$_5$, which should give rise to a negative contribution to the hardness and incompressibility.

In summary, by the first-principles calculations, we have studied the mechanical properties, relative stabilities and electronic structures of diamond, d-BC$_7$ and d-BC$_5$. Our calculated bulk modulus (379–407 GPa), shear modulus (386–410 GPa), elastic constant C$_{44}$ (382–401 GPa), and theoretical hardness (63 GPa) confirm that d-BC$_5$ is an ultraincompressible and superhard material. Also, it exhibits mechanical stability, metallic feature and higher energy barrier than diamond. Furthermore, the trend of mechanical properties for diamond, d-BC$_7$, and d-BC$_5$ has been qualitatively explained. With these physical properties such as exceptional hardness, higher energy barrier than diamond and metallic behavior, this species of d-BC$_x$ materials are attractive for advanced abrasives and high-temperature electronics.

[1] H.-Y. Chung $et~al.$, Science **316**, 436 (2007).
[2] A. Y. Liu and M. L. Cohen, Science **245**, 841 (1989).
[3] D. M. Teter and R. J. Hemley, Science **271**, 53 (1996).
[4] V. L. Solozhenko $et~al.$, Appl. Phys. Lett. **78**, 1385 (2001).
[5] D. He $et~al.$, Appl. Phys. Lett. **81**, 643 (2002).
[6] V. L. Solozhenko $et~al.$, Appl. Phys. Lett. **85**, 1508 (2004).
[7] J. L. He $et~al.$, Appl. Phys. Lett. **88**, 101906 (2006).
[8] P. V. Zinin $et~al.$, J. Appl. Phys. **100**, 013516 (2006).
[9] Y. Zhang $et~al.$, Phys. Rev. Lett. **93**, 195504 (2004).
[10] E. A. Ekimov $et~al.$, Nature (London) **428**, 542 (2004).
[11] J. E. Lowther, J. Phys.: Condens. Matter **17**, 3221 (2005).
[12] S. Chen $et~al.$, Phys. Rev. Lett. **98**, 015502 (2007).
[13] V. L. Solozhenko $et~al.$, Phys. Rev. Lett. **102**, 015506 (2009).
[14] F. Gao $et~al.$, Phys. Rev. Lett. **91**, 015502 (2003).
[15] Z. Fang and K. Terakura, J. Phys.: Condens. Matter **14**, 3001 (2002).
[16] J. P. Perdew and Y. Wang, Phys. Rev. B **45**, 13244 (1992).
[17] J. P. Perdew $et~al.$, Phys. Rev. Lett. **77**, 3865 (1996).
[18] D. Vanderbilt, Phys. Rev. B **41**, 7892 (1990).

[19] H. J. Monkhorst and J. D. Pack, Phys. Rev. B **13**, 5188 (1976).
[20] Y. Liang $et~al.$, Solid State Commun. **146**, 450 (2008).
[21] Y. Liang $et~al.$, Phys. Rev. B **77**, 094126 (2008).
[22] Y. Liang $et~al.$, Phys. Rev. B **79**, 024111 (2009).
[23] M. Calandra and F. Mauri, Phys. Rev. Lett. **101**, 016401 (2008).
[24] T. Shirasaki $et~al.$, Carbon **38**, 1461 (2000).
[25] F. Occelli $et~al.$, Nature Mater. **2**, 151 (2003).
[26] M. Born and K. Huang, $Dynamical~Theory~of~Crystal~Lattices$ (Clarendon, Oxford, 1956).
[27] Y. Liang and B. Zhang, Phys. Rev. B **76**, 132101 (2007).
[28] A. Simunek and J. Vackar, Phys. Rev. Lett. **96**, 085501 (2006).
[29] A. Simunek, Phys. Rev. B **75**, 172108 (2007).
[30] J. C. Boettger, Phys. Rev. B **55**, 11202 (1997).
[31] F. J. Ribeiro $et~al.$, Phys. Rev. B **72**, 214109 (2005).
[32] M. Hanfland $et~al.$, Phys. Rev. B **39**, 12598 (1989).
[33] J. Furthmuller $et~al.$, Phys. Rev. B **50**, 15606 (1994).
[34] J. Sung, J. Mater. Sci. **35**, 6041 (2000).
[35] B. M. Way $et~al.$, Phys. Rev. B **46**, 1697 (1992).
[36] Z. Liu $et~al.$, Phys. Rev. B **73**, 172101 (2006).